IOP FTC
IOP PUBLISHING JOURNAL OF PHYSICS B: ATOMIC, MOLECULAR AND OPTICAL PHYSICS
J. Phys. B: At. Mol. Opt. Phys. **41** (2008) 101001 (7pp) doi:10.1088/0953-4075/41/10/101001

FAST TRACK COMMUNICATION

Angular momentum of photons and phase conjugation

A Yu Okulov

General Physics Institute of Russian Academy of Sciences, Vavilova street 38, 119991, Moscow, Russia

E-mail: okulov@kapella.gpi.ru

Received 27 December 2007, in final form 19 March 2008
Published 6 May 2008
Online at stacks.iop.org/JPhysB/41/101001

Abstract

Using the concept of an *ideal* phase-conjugating mirror we demonstrate that regardless of internal physical mechanism the phase-conjugation of a singular laser beam is accompanied by excitation within the mirror of internal waves which carry doubled angular momentum in order to match angular momentum conservation. For a Brillouin hypersound wavefront-reversal mirror this means that each elementary optical vortex belonging to a speckle pattern emits an acoustical vortex wave with doubled topological charge. The exact spatial profiles of light intensity and the intensity of hypersound in the vicinity of the phase singularity are obtained. These *spiral* profiles have a form of double helix which rotates with the frequency of sound. An optoacoustic experiment is proposed for visualization of the wavefront reversal of twisted optical beams and tunable twisted sound generation.

The conservation of angular momentum (AM) $\vec{J}$ stems from the isotropy of space [1]. In contrast to particles with nonzero rest mass m_o, the decomposition of $\vec{J}$ into 'spin' $\vec{S}$ and 'orbital' $\vec{L}$ parts of a photon's AM is referred to as an ambiguous procedure [1, 2]. The spin part $\vec{S}$ is related to polarization, i.e. time-dependent layout of electrical $\vec{E}$ and magnetic $\vec{B}$ fields of the 'transverse' light wave. The orbital part (OAM) $\vec{L}$ is associated with a helical staircase wavefront [2–5]. As a matter of fact purely transverse light waves are an abstraction because of small but inevitable projections of $\vec{E}$ and $\vec{B}$ in the direction of propagation, say the z-axis (figure 1). Indeed, the spin-orbital coupling of light occurs [6] due to a vectorial interplay between longitudinal and transversal components of the fields $\vec{E}$ and $\vec{B}$. The vectorial solutions of Maxwell's equations for propagation of light spatially localized by a waveguide or emitted through a finite aperture to free space give a strict relationship between the longitudinal and transversal field components [7, 8]. Nevertheless the approximate decomposition in the form $\vec{J} = \vec{S} + \vec{L}$ has proven to be very fruitful for small curvatures of the light wavefront, i.e. in the paraxial wave approximation [2].

The propagation of light in an anisotropic medium changes the polarization, and historically the spin of photon was observed for the first time in Bethe's experiment where a birefringent $\lambda/2$ plate induced a change of photon polarization from circular ($S_z = +\hbar$) to counter-rotating ($S_z = -\hbar$) [9]. The elementary event of the photon's spin change is accompanied by a back action and a stepwise change in the angular momentum of a plate. The quantum–classical correspondence is fulfilled by the origin of a macroscopically observable classical torque $\vec{T} = \frac{\mathrm{d}}{\mathrm{d}t}\vec{J} = [\vec{D} \times \vec{E}]$ [2], where $|\vec{J}| \approx \frac{I}{\omega}$, ω is angular frequency and I the intensity of light.

The reflection of a circularly polarized photon from an ideal conventional mirror (metal of multilayer dielectric) does not change the direction of both the spin $\vec{S}$ and orbital momentum $\vec{L}$ in the laboratory frame, and the mechanical torque $\vec{T}$ on such a mirror is absent (figure 1). This follows from both the boundary conditions for Maxwell's equations [8] and rotational symmetry of the setup with respect to the z-axis [1, 10].

The current communication pays particular attention to conservation laws for reflection of a photon carrying OAM $L_z = \ell\hbar$ from a phase-conjugating mirror (PCM). The discussion is centered mainly around a Brillouin wavefront-reversal mirror [10]. We will demonstrate the hidden anisotropy of an SBS-mirror which arises due to excitation of internal helical waves, i.e. acoustical vortices, whose existence

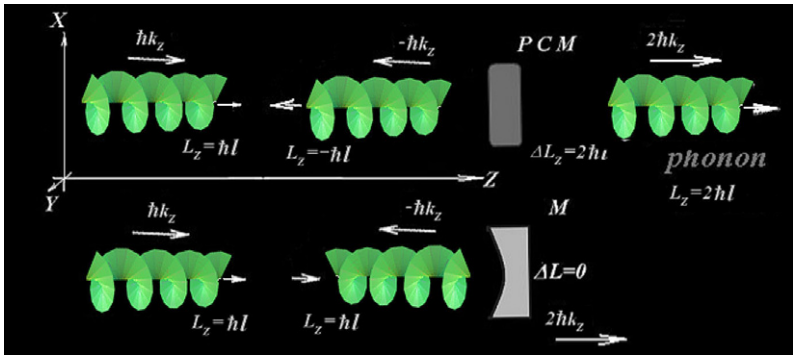

Figure 1. The comparison between a conventional mirror (M, bottom) and a wavefront reversal mirror (PCM, upper) from the point of view of angular momentum transformation in the photon's reflection. Upper view: the 'right' photon with plane polarization and helical wavefront strikes the PCM and decays to the 'right' photon, moving in the opposite direction with momentum $-\hbar k_z$. The acoustical phonon absorbs translational in the recoil momentum $2\hbar k_z$ and rotational recoil OAM $2\hbar$. Bottom view: the 'right' photon with topological charge +1 strikes the conventional mirror M and transforms to 'left' photon. In this case the OAM is not changed and the rotational recoil is absent.

was proven recently for MHz-range sound [11]. The rotation of ultracold cesium atoms [12] was also suggested to occur because of the OAM transfer due to backward reflection of a Laguerre–Gaussian beam (LG) with 0.001 diffractive efficiency via a nondegenerate four-wave mixing process. The OAM transfer from co-propagating circularly polarized LG to BEC [13] has also been discussed.

The circularly polarized photon is called 'right' when the projection of spin S_z onto the direction of propagation is positive (figure 1). This happens for example, when the photon moves in the positive direction of the z-axis with momentum $\hbar\vec{k}$, and fields $\vec{E}$ and $\vec{B}$ rotate clockwise with respect to $\vec{k}$. In contrast the 'left' photon has counter-clockwise rotation of the polarization and carries spin $S_z = -\hbar$.

When reflecting from a conventional mirror the incident 'right' photon with $S_z = +\hbar$ and momentum $p_z \approx \hbar|\vec{k}|$ moving in the positive direction of the z-axis is transformed into a 'left' photon having $p_z \approx -\hbar|\vec{k}|$ and the same spin projection $S_z = +\hbar$. And vice versa, when the incident 'left' (or counter-clockwise) photon strikes the mirror, the sign of $S_z = -\hbar$ does not change in the laboratory frame and the photon becomes 'right'. This is not surprising because the setup is isotropic. In this situation the only mechanical effect on the mirror is light pressure [14, 15], whose major component is normal to the mirror surface. So the conventional mirror in *normal* reflection accepts momentum $\Delta p_z \approx 2\hbar\vec{k}$ as a single entity and does not change both the polarization (or spin $\vec{S}$) and orbital momentum $\vec{L}$.

The situation changes drastically for the PCM [10]. The conservation laws determine the energy of the excited acoustical photon $\hbar\Omega_a$ as the difference between the energies of the incident $\hbar\omega_p$ and reflected $\hbar\omega_s$ photons. The radiation pressure also occurs here because of the net momentum transfer to sound $p_{\text{phonon}} = \Delta p_z \approx 2\hbar k_z$ or 'recoil'. The most interesting feature is the conservation of OAM $\vec{L}$. Let us show that the wavefront-reversal mirror should feel the 'rotational recoil' when the vortex beam carrying OAM is reflected with ultimate phase conjugation fidelity. Indeed, because of the basic feature of phase-conjugation the retroreflected photon passes all states of the incident one in a reverse sequence [16]. This is the so-called time reversal property of the wavefront-reversing mirror. Consequently the helicoidal phase surfaces of the incident photon and reflected photon should be matched perfectly (figure 1). The small mismatch of the wavefronts caused by recoil frequency shift and wavenumber shift of the order 10^{-5} [16] does not affect the phase surfaces. Because of an accurate wavefront match the OAM is turned 180° and the OAM projection $L_z = +\ell\hbar$ is changed to the opposite one $L_z = -\ell\hbar$. As a consequence the 'winding' number or topological charge ℓ does not change sign with respect to the propagation direction $\vec{k}$. Thus the conjugated photon with 'right' OAM remains 'right', and the photon with 'left' OAM remains 'left'.

The apparent physical consequence of this fact is the necessity of the excitation of the *internal wave* which ought to absorb the difference between angular momenta $\Delta L_z = +2\ell\hbar$ before and after the retroreflection. Consequently this internal wave should have a singular wavefront provided the PCM is ideal. At this point let us stress again the remarkable difference between the spin $\vec{S}$ and orbital $\vec{L}$ components of the angular momentum. The electrostrictive nonlinearity in an isotropic medium is scalar in the paraxial approximation at least, and the spin part of AM is not turned to the opposite one [10]. In contrast, the orbital component $\vec{L}$ of OAM does turn, because acoustical vortices do exist [11]. It will be shown below in detail by exact analytical formulas that acoustical vortices absorb the OAM. In fact there exist some obstacles to the realization of the perfect phase-conjugation of elementary optical vortices, say in the form of LG [17]. Nevertheless it will be shown below how to overcome this class of difficulties using traditional and reliable methods of the Brillouin phase-conjugation [16].

For this purpose let us separate the region of wavefront reversal via traditional phase-conjugating mechanisms, e.g. Brillouin PCM and optoacoustic cell (OA) where sound is excited parametrically, without a reverse action on light (figure 2). This geometry makes possible in visualizing inside the OA acoustical vortex collocated with the optical phase singularity in a spatial region having size up to several millimeters in transverse dimensions, i.e. in the x, y-plane [11].

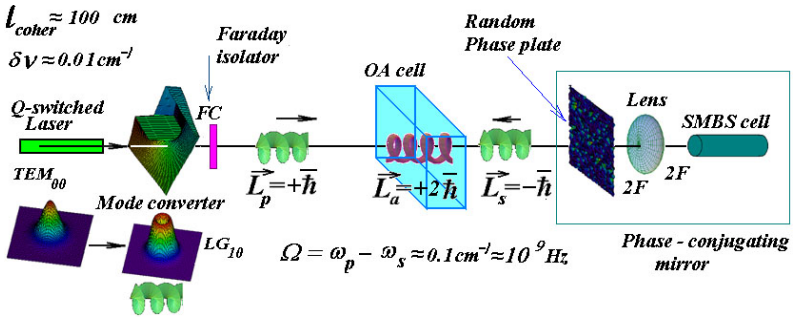

Figure 2. The proposal for the experimental setup for twisted hypersound observation. The laser field E_p comes through the mode converter and Faraday cell (FC) to the optoacoustic cell OA. The transparent random phase plate is used for initiation of a high-fidelity phase-conjugation in the multimode the Brillouin-active waveguide SBS. F is the focal distance of the lens. The phase conjugated Stokes field E_s interferes with the pump field E_p inside OA to produce a rotating spiral interference pattern of transverse size of several millimeters. The twisted sound phonons excited by counter-propagating fields are expected to have OAM $L_a = 2\hbar$ directed to the right. The angular speed of rotation is equal to acoustical frequency $\Omega_a \approx 10^9$ Hz.

The acoustical waves inside Brillouin PCM volume are highly dissipative, because hypersound has a typical relaxation time of about 10^{-9} s [10]. In liquid crystals, which are used for phase-conjugation, the relaxation time is significantly longer -10^{-3} s [10]. In the second case one might expect to observe the macroscopic torque on PCM for appropriate time scales. In contrast, in an anisotropic artificial medium like Veselago's lens [18] there might appear a macroscopic rotational recoil caused by optical torque.

Consider for definiteness the interaction between the two counter-propagating paraxial laser beams inside the Brillouin active medium. Instead of the quantized field description by means of Heisenberg's secondary-quantization $\hat{\Psi}$-operators [1] we choose a more intuitive approach of using classical counter-propagating optical fields $\mathbf{E_p}$, $\mathbf{E_s}$ and acoustic field $\mathbf{Q}$. The linearly polarized 'pump' field $\mathbf{E_p}$ moves in the positive direction of the z-axis; the reflected Stokes field $\mathbf{E_s}$ with the same polarization propagates in the opposite direction (figure 3). The acoustic field $\mathbf{Q}$ is excited via electrostriction. The cylindrical system of coordinates (z, r, ϕ, t) is chosen for the equations below. The connection with Cartesian coordinates used in figures is supposed to be evident. The 'parabolic' equations of motion are well known [10]. The 'envelope' complex amplitude of pump wave E_p moving from left to right (figure 1) follows:

$$\frac{\partial E_p(z,r,\phi,t)}{\partial z} + \frac{n}{c}\frac{\partial E_p}{\partial t} + \frac{\mathrm{i}}{2k_p}\Delta_\perp E_p = \frac{\mathrm{i}\gamma\omega_p}{4\rho_0 nc} Q E_s, \quad (1)$$

The Stokes wave 'envelope' E_s moving from right to left is controlled by:

$$\frac{\partial E_s(z,r,\phi,t)}{\partial z} - \frac{n}{c}\frac{\partial E_s}{\partial t} - \frac{\mathrm{i}}{2k_s}\Delta_\perp E_s = -\frac{\mathrm{i}\gamma\omega_s}{4\rho_0 nc} E_p Q^*, \quad (2)$$

The acoustic wave 'envelope' Q moving from the left to right obeys:

$$v_a \frac{\partial Q(z,r,\phi,t)}{\partial z} + \frac{\partial Q}{\partial t} + \frac{\Gamma Q}{2} = \frac{\mathrm{i}\gamma k_a{}^2}{16\pi\Omega_a} E_p E_s{}^*, \quad (3)$$

where $\gamma = \rho(\partial\epsilon/\partial\rho)$ is the electrostrictive coupling constant, ρ_0 is the density of medium, n is the index of refraction, c is the speed of light, and v_a is the speed of sound [19]. The connections between 'envelope' complex amplitudes

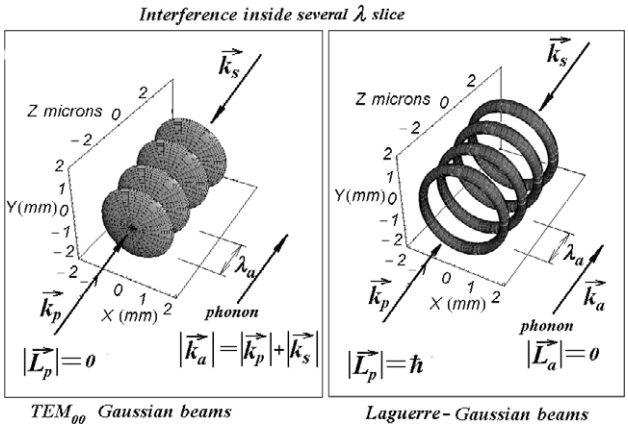

Figure 3. Interference pattern of the incident (pump) Gaussian mode wave E_p with field E_s reflected from a conventional mirror. Left: incident zeroth-order Gaussian beam forms moving in a quasi-sinusoidal pattern with period $\lambda/2$ due to interference with the reflected beam. Four isosurfaces of interference maxima are shown. The direction of pattern motion is changed as the sign of Ω changes. The pattern is the same for a reflecting TEM_{oo} beam from M and PCM. The period of acoustical grating is equal roughly to half of the pumping wavelength satisfying the Bragg reflection condition. Right: LG beam interferes with LG reflected from a conventional mirror. A sequence of toroidal rings occurs. The OAM is not transferred to the medium.

E_p, E_s, Q and field amplitudes $\mathbf{E_p}$, $\mathbf{E_s}$ and $\mathbf{Q}$ are given by [10, 19]:

$$\begin{aligned} \mathbf{E_p} &= \exp[\mathrm{i}(+k_p z - \omega_p t)] E_p(z,r,\phi,t); \\ \mathbf{E_s} &= \exp[\mathrm{i}(-k_s z - \omega_s t)] E_s(z,r,\phi,t) \\ \mathbf{Q} &= \exp[\mathrm{i}(+k_a z - \Omega_a t)] Q(z,r,\phi,t) \end{aligned} \quad (4)$$

Equations (1)–(3) are valid within both the Brillouin mirror and OA (figure 2). The solution of (1)–(3) for OA could be obtained under the natural physical assumption that amplitudes $\mathbf{E_p}$ and $\mathbf{E_s}$ are small enough and the acoustic field Q is excited parametrically, by electrostrictive force in the right-hand side of (3). This assumption enables us to solve (1)–(2) for the free-space approximation, i.e. without involving right-hand sides.

For a Cauchy problem with a first-order LG beam as initial condition for $\mathbf{E_p}$ (from left window of OA) and $\mathbf{E_s}$ (from right window of OA) we have the following *exact* solutions for the pump field $\mathbf{E_p}$:

$$\mathbf{E_p}(z,r,\phi,t) \sim \frac{E_p^o \exp[\mathrm{i}(+k_p z - \omega_p t) + \mathrm{i}\ell\phi]}{(1+\mathrm{i}z/(k_p D^2))^2} r^\ell \times \exp\left[-\frac{r^2}{D^2(1+\mathrm{i}z/(k_p D^2))}\right], \quad (5)$$

and for the Stokes field $\mathbf{E_s}$:

$$\mathbf{E_s}(z,r,\phi,t) \sim \frac{E_s^o \exp[\mathrm{i}(-k_s z - \omega_s t) \pm \mathrm{i}\ell\phi]}{(1+\mathrm{i}z/(k_s D^2))^2} r^\ell \times \exp\left[-\frac{r^2}{D^2(1+\mathrm{i}z/(k_s D^2))}\right]. \quad (6)$$

The fields $\mathbf{E_p}$ and $\mathbf{E_s}$ carry angular momentum $\ell\hbar$ per photon [5], where ℓ is the above-mentioned 'topological charge' or 'winding number', D is the diameter of the beam 'necklace' at full width half-maximum (FWHM), z is distance passed along the z-axis from the beam necklace, $r = |\vec{r}|$ the length of the radius vector perpendicular to z-axis, ϕ the azimuthal angle, E_s^o and E_p^o are the maximal electrical field amplitudes in the necklace. The maximally simplified form of the free-space solution chosen for LG [20] under the assumption that the Fresnel number for OA is large enough $N_f = k_{p,s} D^2/z \gg 1$, or the thickness of OA is much shorter than the Rayleigh range $k_{p,s} D^2$.

Consider first the interference patterns produced by two counter-propagating fields $\mathbf{E_p}$ and $\mathbf{E_s}$ with equal amplitudes $E_{p,s}^o$ and without phase singularities, i.e. two zeroth-order Gaussian beams or TEM_{oo}-beams near their overlapping necklaces:

$$\mathbf{E}_{(p,s)}(z,r,\phi,t) \approx E_{p,s}^o \exp\left[-\mathrm{i}\omega_{(p,s)}t \pm \mathrm{i}k_{(p,s)}z - \frac{r^2}{D^2(1 \pm \mathrm{i}z/(k_{(p,s)}D^2))}\right] \quad (7)$$

The isosurfaces of intensity $I_{\text{surface}} < 2|E_0|^2$ as functions of cylindrical coordinates (z,r,ϕ,t) are solutions of the following *implicit* equation reminiscent of a basic course of physical optics:

$$\mathbf{I}_{\text{isosurface}} = |\mathbf{E}(z,r,\phi,t)|^2 = |\mathbf{E}_p(z,r,\phi,t) + \mathbf{E}_s(z,r,\phi,t)|^2 \cong 2\left|E_{p,s}^o\right|^2 [1 + \cos[(\omega_p - \omega_s)t - (k_p + k_s)z]] \times \exp\left[-\frac{2r^2}{D^2\left(1 + z^2/\left(k_p^2 D^4\right)\right)}\right]. \quad (8)$$

In addition to the familiar interference term $\cos[(\omega_p - \omega_s)t + (k_p + k_s)z]$ which describes a grating with period $\mathcal{P} = 2\pi(k_p + k_s)^{-1}$ moving along the z-axis with acoustical speed $v_a = [(\omega_p - \omega_s)/(k_p + k_s)]$, a Gaussian function arises which modulates the *rolls* of the interference pattern in the transverse direction. Thus the isosurfaces of intensity are pancake-like *rotational ellipsoids* separated by distance $\mathcal{P}$ (figure 3). Such an interference pattern is in strict agreement with Doppler's mechanism of Brillouin scattering: the pump field is being reflected from the grating which moves with speed v_a. The resulting Doppler shift $\omega_p - \omega_s$ is such that the optical interference pattern perfectly overlaps with the spatial profile of the acoustic field. The left picture of figure 3 illustrates this moving interference pattern for four periods. In a conventional picture of stimulated Brillouin scattering this moving pattern coincides with the moving profile of a hypersound wave [10]. The spatial period of this wave $\mathcal{P} = \lambda_a = 2\pi/(k_p + k_s)$ is such that the Bragg condition for normal reflection from the moving grating $((\lambda_p)^{-1} + (\lambda_s)^{-1} = (\lambda_a)^{-1})$ is satisfied.

Suppose now that first-order LG is reflected from a conventional, non-phase-conjugating parabolic mirror (figure 1). Because orbital angular momentum is not changed in such reflection in the laboratory frame, the helical terms $(\ell\phi)$ have identical signs in the expressions for fields $\mathbf{E_p}$ and $\mathbf{E_s}$:

$$\mathbf{E}_{(p,s)}(z,r,\phi,t) \approx E_{p,s}^o r^\ell \exp[-\mathrm{i}\omega_{(p,s)}t \pm \mathrm{i}k_{(p,s)}z + \mathrm{i}\ell\phi] - \left[\frac{r^2}{(D^2(1 \pm \mathrm{i}z/(k_{(p,s)}D^2)))}\right] \quad (9)$$

Then two counter-propagating first-order LG produce in OA a more complicated interference pattern, with a *hole* on the beam axis. As a result, instead of a sequence of ellipsoids we have a sequence of toroidals separated by period $\lambda_a = 2\pi(k_p + k_s)^{-1}$ fulfilling the Bragg resonant condition (figure 3):

$$\mathbf{I}_{\text{isosurface}} = |\mathbf{E}(z,r,\phi,t)|^2 = |\mathbf{E}_p(z,r,\phi,t) + \mathbf{E}_s(z,r,\phi,t)|^2 \approx 2\left|E_{p,s}^o\right|^2 [1 + \cos[(\omega_p - \omega_s)t - (k_p + k_s)z]] r^\ell \times \exp\left[-\frac{2r^2}{D^2(1 + z^2/(k_p^2 D^4))}\right]. \quad (10)$$

Again the interference pattern moves along the z-axis with acoustic speed v_a. The direction of motion is determined by the sign of the difference $(\omega_p - \omega_s)$. For the anti-Stokes difference between frequencies the interference pattern moves in the negative direction of the z-axis.

Phase conjugation of LG changes the interference pattern drastically. Because orbital angular momentum changes to the opposite one in the wavefront reversal process, the helical terms $\ell\phi$ have opposite signs in the expressions for fields $\mathbf{E_p}$ and $\mathbf{E_s}$, which read:

$$E_{(p,s)}(z,r,\phi,t) \approx E_{p,s}^o r^\ell \exp[-\mathrm{i}\omega_{(p,s)}t \pm \mathrm{i}k_{(p,s)}z \pm \mathrm{i}\ell\phi] - \left[\frac{r^2}{(D^2(1 \pm \mathrm{i}z/(k_{(p,s)}D^2)))}\right] \quad (11)$$

This mathematical peculiarity, namely $\pm$ before azimuthal angle ϕ, follows from the physical fact that after retroreflection the ideally phase-conjugated wave passes all states of the incident wave in a reverse sequence ([16]). As a result the expression for the interference pattern is slightly different:

$$\mathbf{I}_{\text{isosurface}} = |\mathbf{E}(z,r,\phi,t)|^2 = |\mathbf{E}_p(z,r,\phi,t) + \mathbf{E}_s(z,r,\phi,t)|^2 \approx 2\left|E_{s,p}^o\right|^2 [1 + \cos[(\omega_p - \omega_s)t - (k_p + k_s)z + 2l_w\phi]] r^{2l_w} \times \exp\left[-\frac{2r^2}{D^2\left(1 + z^2/\left(k_p^2 D^4\right)\right)}\right]. \quad (12)$$

The self-similar variable $(\omega_p - \omega_s)t - (k_p + k_s)z$ in the argument of cos acquires the doubled azimuthal angle $2\ell\phi$. As a consequence the interference pattern changes from

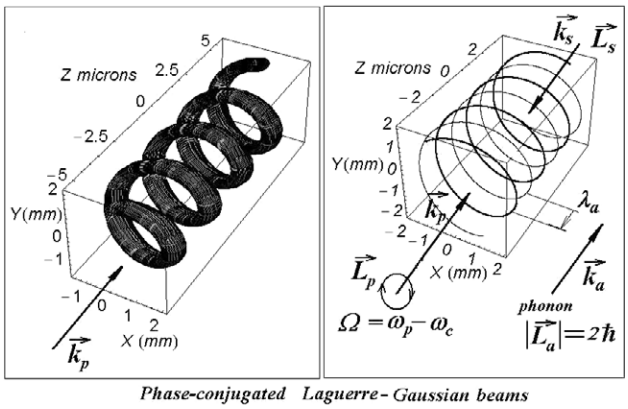

Figure 4. Interference pattern of incident 'right' (pump) first-order LG wave E_p and phase-conjugated 'right' replica E_s. The topological charge is $\ell = +1$. Left: the spiral distribution of intensity occurs. Only a single string is shown because of computational limitations. Right: actually the interference pattern has the form of a double helix. The right plot depicts the maxima of the intensity only. The double helix rotates clockwise when the frequency difference is positive (Stokes case). For anti-Stokes retroreflection the rotation of helix is counter-clockwise. The period of the acoustical spring is roughly half of the pumping wavelength for Brillouin scattering.

a sequence of toroidal rings to a double helix (figure 4). The spiral interference pattern has *two maxima* because the azimuthal dependence contains the doubled azimuthal angle ϕ. The spatial period of the springs is again automatically adjusted in such a way that one may say the generalized Bragg condition is satisfied. The other drastic feature is that the interference pattern rotates with angular velocity equal to the acoustical frequency $\Omega_a = (\omega_p - \omega_s)$. The linear translational speed of z-aligned motion of a helix's turns is exactly equal to the sonic speed v_a:

$$v_a = \frac{(\omega_p - \omega_s)}{(k_p + k_s)} \tag{13}$$

Similar double-helix structures were reported recently for Wigner crystals in a dusty plasma [21].

The singular acoustical fields in the MHz-range were generated and measured [11] and the helical acoustical wavefronts were recorded. Let us obtain the exact expression for spatial distribution of the sound intensity near the optical phase singularity in a Brillouin medium using the equation for the acoustical field (3). The expression for intensity of a hypersound field I_{sound} reads immediately from the general expressions for electrostrictive nonlinearity [10, 19]:

$$\mathbf{I}_{\text{sound}} \approx |\mathbf{E}(z, r, \phi, t)|^2 = \left|E^o_{p,s}\right|^2 [1 + \cos[(\omega_p - \omega_s)t - (k_p + k_s)z + 2\ell\phi]] \, r^{2\ell} \exp\left[-\frac{2r^2}{D^2(1 + z^2/(k_p^2 D^4))}\right]. \tag{14}$$

We designate this acoustic vortex field as $\mathbf{Q}_{\text{twisted}}$ having in mind the helical distribution of intensity (figure 4). It is clear that such a vortex possesses *doubled* angular momentum, as is seen from the doubled azimuthal angle $2\ell\phi$ in the self-similar argument of cos in (14). In addition the complex acoustic envelope Q_{twisted} could be derived in the steady-state regime due to the fact of the strong dumping of the acoustical field. The lifetime of the hypersound wave Γ^{-1} is of the order of several nanoseconds in typical liquid and gaseous media [10]. Thus the expression for the acoustical envelope Q_{twisted} is obtained in steady-state from (3) using (9):

$$Q_{\text{twisted}} \approx E_p E_s{}^* \approx \exp[+\mathrm{i}2\ell\phi] r^{2\ell} \times \exp\left[-\frac{2r^2}{D^2\left(1 + z^2/\left(k_p^2 D^4\right)\right)}\right]. \tag{15}$$

Evidently the envelope of the acoustic wave Q_{twisted} has a helical wavefront with doubled topological charge 2ℓ. The twisted spatiotemporal acoustic field $\mathbf{Q}_{\text{twisted}}$ has the following form:

$$\mathbf{Q}_{\text{twisted}} \approx \mathbf{E}_p \mathbf{E}_s{}^* \approx \exp[\mathrm{i}(\omega_p - \omega_s)t - \mathrm{i}(k_p + k_s)z + \mathrm{i}2\ell\phi] \times r^{2\ell} \exp\left[-\frac{2r^2}{D^2\left(1 + z^2/\left(k_p^2 D^4\right)\right)}\right]. \tag{16}$$

The phase dislocation of the acoustic wave rotates with acoustical frequency $\Omega_a = \omega_p - \omega_s$. The speed of translational motion in the z-direction of the rotating turns of an acoustical spring is exactly equal to the speed of sound v_a. The rotating spring could be visualized by currently available experimental tools [11], because the transverse size of the beam necklace could easily be changed, e.g. by additional lenses.

The previous exact expressions (12), (14) and (16) are based upon elementary exact solutions of the parabolic wave equations in the form of the first-order LG. This simplification became possible due to geometrical separation of the OA with weak interaction between counter-propagating beams from PCM where strong interaction between the optical fields $\mathbf{E_p}$ and $\mathbf{E_s}$ takes place. The straightforward generalization is to be made taking into account the *elongated geometry* of phase singularities inside the speckle pattern within the SBS-mirror volume (figure 2) [10]. The expression for optical fields near the phase singularity with topological charge ℓ could be generalized in the following form:

$$\mathbf{E}_{(p,s)}(z, r, \phi, t) = E^o_{p,s} r^{\ell} \times \exp[-\mathrm{i}\omega_{(p,s)}t \pm \mathrm{i}k_{(p,s)}z \pm \mathrm{i}\ell\phi]] f(r, z), \tag{17}$$

where $f(r, z)$ is a smooth function elongated in the z-direction. The inequality between the forward E_p and backward E_s fields amplitudes does not affect qualitatively the helical interference patterns (figure 4) in the regime of weak saturation, because the Brillouin wavefront reversal mirrors with random phase plate have sufficiently high (approximately 0.9) phase-conjugating fidelity [16]:

$$K = \frac{\left|\int \mathbf{E}_p \mathbf{E}_s^* \, \mathrm{d}\vec{r}\right|^2}{\left(\int |\mathbf{E}_p|^2 \, \mathrm{d}\vec{r}\right)\left(\int |\mathbf{E}_s|^2 \, \mathrm{d}\vec{r}\right)}, \tag{18}$$

The experimentally verified procedure utilizes thin transparent glass plates with chaotic phase modulation (figure 2) which have transverse correlation length of about tens of microns. Such geometry looks promising for realization of the phase-conjugation of LG and in overcoming the difficulties reported earlier [17]. Because of the high degree of phase-conjugation fidelity of the forward $\mathbf{E}_p$ and

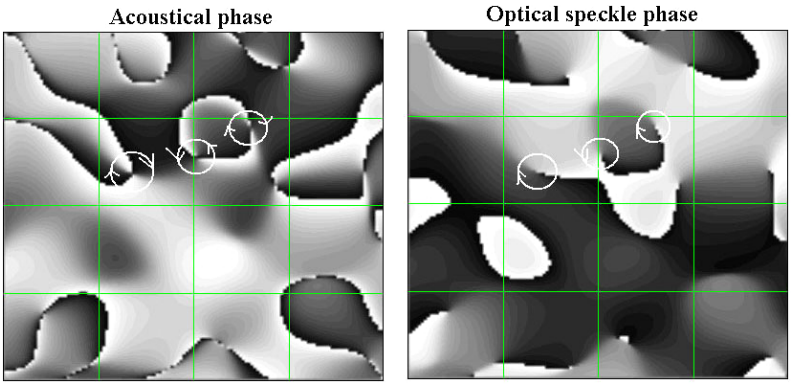

Figure 5. A comparison between acoustical (left) and optical *speckle* (right) fields inside the Brillouin mirror pumped by a multimode random phase field. The optical vortices on the right panel are designated by white circles with one arrow. The phase is changed from 0 to $\pm 2\pi$ in motion around the optical phase singularity. The collocated acoustical vortices on the left panel are shown by white circles with two arrows. The phase is changed from 0 to $\pm 4\pi$ in motion around the acoustical phase singularity. The transverse X, Y scale is $100 \times 100\,\mu$m.

backward $\mathbf{E}_s$ fields one may consider transverse distributions of pump and Stokes fields near the entrance window of PCM as almost identical. Thus the above expressions (12), (14) and (16) for spring interference patterns might be valid for speckle fields as well. This enables us to plot transverse distributions of the optical and acoustical phases in the output planes of the PCM and OA in a similar way, where the phase-conjugated Stokes field $\mathbf{E_s}$ is in good correlation with the pump field $\mathbf{E_p}$. Choosing the 8×8 random plane wave superposition for $\mathbf{E_p}$ and $\mathbf{E_s} \approx \mathbf{E_p^*}$, we obtained using (15) the transverse distributions of the phase of the envelope of the optical speckle field $arg(E_p(\vec{r}_\perp))$ and for the envelope of a field of collocated acoustical vortices $arg(Q_{\text{twisted}}(\vec{r}_\perp))$. The acoustical vortices have doubled topological charges (figure 5).

In summary we demonstrated that wavefront reversal mirrors are chiral optical antennas. The elementary consideration of conservation laws including conservation of AM shows the existence of twisted rotating structures inside an ideal phase-conjugator. For a stimulated Brillouin scattering mirror the rotating spiral interference pattern modulates the dielectric permittivity ϵ via electrostriction. The dynamical equations give exact expressions for sound intensity inside the acoustical phase singularity which is collocated with the optical phase singularity. It is worth mentioning that the above-presented model does not take into account several essential features of the Brillouin PCM, e.g. longitudinal dependence of optical fields and corresponding spatial mismatch of their amplitudes. The reflection of the both elementary optical vortices like LG and speckle fields is also accompanied by excitation inside the SBS wavefront-reversal mirror of *sonic* vortices with doubled topological charge. Internal helical waves and spiral modulation of dielectric permittivity induce local anisotropy inside the phase-conjugating mirror and force the exchange of angular momentum. A new experimental geometry is proposed (figure 2) in order to observe parametric excitation of isolated acoustical vortices inside the OA. The interference pattern near each phase singularity in a speckle pattern rotates clockwise with angular speed $\Omega = \omega_p - \omega_s$ regardless of the sign of spirality of the interference spring. The rotation changes direction to counter-clockwise for all singularities in a speckle for anti-Stokes frequency of the retroreflected wave. The angular speed Ω depends also on the physical mechanism of the wavefront reversal. It could span from units of Hz for the photorefractive crystals to the range of THz for Raman phase-conjugators [10].

The connection between the angular momenta of the incident and reflected photons seems to be valid for any other nonlinear PCM including the photorefractive one. In order to transfer OAM the rotating intensity springs should excite the helical waves intrinsic to the given type of phase-conjugating mirror. The peculiarities of photorefractive media, e.g. nonstationary vortex reflection, screening, vortex splitting and 'disappearance of nonlinearity' [22] also deserve special attention. The successful wavefront reversal of complex images obtained from the first experiments with photorefractive phase conjugators [23] is indirect evidence for the existence of internal helical waves in the volume of photorefractive PCM and other phase-conjugators such as liquid-crystal light valves.

The correspondence between formulas for classical fields $\mathbf{E_p}, \mathbf{E_s}$ and $\mathbf{Q}$ and quantum field description by means of Heisenberg's secondary-quantization $\hat{\Psi}$-operators [1] will be given elsewhere. Briefly, in the quantum picture of ideal phase conjugator (figure 1) each incident photon with orbital angular momentum $L_z = \ell\hbar$ decays to a reflected photon with opposite $L_z = -\ell\hbar$ projection on the propagation axis and a quantum of internal wave with doubled OAM $L_z^a = 2\ell\hbar$.

References

[1] Lifshitz E M, Pitaevskii L P and Berestetskii V B 1982 *Quantum Electrodynamics (Landau and Lifshitz Course of Theoretical Physics* Vol 4*)* (Oxford: Butterworth-Heineman) Ch. I, section 6, 8
[2] Allen L, Beijersbergen M W, Spreeuw R J C and Woerdman J P 1992 *Phys. Rev.* A **45** 8185–9
[3] Nye J F and Berry M V 1974 *Proc. R. Soc. London Ser.* A **336** 165
[4] Soskin M S and Vasnetsov M V 2001 *Progress in Optics* vol 42 ed E Wolf (Amsterdam: Elsevier) pp 219–76
[5] Leach J, Padgett M J, Barnett S M, Franke-Arnold S and Courtial J 2002 *Phys. Rev. Lett.* **88** 257901

[6] Liberman V S and Zeldovich B Ya 1992 *Phys. Rev.* A **46** 5199
[7] Jackson J D 1962 *Classical Electrodynamics* (New York: Wiley)
[8] Weinstein L A 1969 *Open Resonators and Open Waveguides* (Boulder, CO: Golem)
[9] Beth R A 1936 *Phys. Rev.* **50** 115
[10] Zeldovich B Y, Pilipetsky N F and Shkunov V V 1985 *Principles of Phase Conjugation* (Berlin: Springer)
[11] Thomas J-L and Marchiano R 2003 *Phys. Rev. Lett.* **91** 244302
[12] Petrov D V and Tabosa J W R 1999 *Phys. Rev. Lett.* **83** 4967
[13] Marzlin K-P, Zhang W and Wright E M 1997 *Phys. Rev. Lett.* **79** 1997
[14] Lebedev P N 1901 *Ann. Phys., Lpz.* **6** 433
[15] Friese M J, Euger J and Rubinstein-Dunlop H 1996 *Phys. Rev.* A **54** 1543
[16] Basov N G, Zubarev I G, Mironov A B, Mikhailov S I and Okulov A Y 1980 *JETP* **52** 847
[17] Starikov F A, Dolgopolov Yu V, Kopalkin A V, Kochemasov G G, Kulikov S M and Sukharev S A 2006 *J. Phys. IV France* **133** 683–5
[18] Veselago V G 1968 *Sov. Phys.—Usp.* **10** 509
[19] Boyd R W, Rzazewsky K and Narum P 1990 *Phys. Rev.* A **42** 5514
[20] Okulov A Yu 2008 *J. Mod. Opt.* **55** 241–57
[21] Tsytovich V N 2007 *Phys.—Usp.* **50** 409
[22] Mamaev A V, Saffman J and Zozulya A A 1996 *Phys. Rev.* A **56** R1713
[23] Feinberg J and Hellwarth R W 1981 *Opt. Lett.* **6** 257